Journal of Bioscience and Bioengineering
VOL. 127 No. 6, 714–720, 2019

www.elsevier.com/locate/jbiosc

Exoelectrogenic response of *Pichia fermentans* influenced by mediator and reactor design

Mamta Pal and Rakesh Kumar Sharma*

Department of Biosciences, Manipal University Jaipur, Jaipur 303007, Rajasthan, India

Received 11 August 2018; accepted 7 November 2018
Available online 11 December 2018

Microbial fuel cell is one of the most convenient and cost-effective technology for producing the clean energy. This study explores the exoelectrogenic behavior of *Pichia fermentans* in a microbial fuel cell. Two different reactor designs (double- and single-chambered) were tested in the presence and in the absence of a mediator (methylene blue). The influence of extracellular polymeric substances in the electricity generation has also been studied. In a double-chambered setup, maximum open circuit voltages were measured as 0.602 and 0.488 V with mediator and without mediator cell, respectively, whereas maximum power densities were measured as 1.23 μWcm^{-2} and 0.407 μWcm^{-2}, respectively. In addition, maximum open circuit voltages were observed as 0.40 and 0.397 V in a single-chambered fuel cell with and without mediator, respectively. The maximum power density was recorded 1.64 μWcm^{-2} in the presence of a mediator, whereas the same was found as 0.643 μWcm^{-2} in the absence of mediator. Thus, these results indicate that *P. fermentans* has the ability to produce high power density under microaerophilic conditions with mediator in a single-chambered membrane less setup.

[**Key words:** Microbial fuel cell; *Pichia fermentans*; Extracellular polymeric substances; Methylene blue; Single-chambered cell]

Microbial fuel cell (MFC) directly converts chemical energy of organic waste into electricity using microorganism as a biocatalyst. In this device, microbial metabolites play significant role in the electrochemical reactions responsible for the electron transport. It is a promising technology that can be used for electricity generation, wastewater treatment, bioremediation of heavy metals/toxic compounds (1). MFC is a simple, easy to operate device that can work efficiently even at low temperatures without any external energy input (2). MFCs are usually evaluated by their power generation capacity, columbic efficiency, stability, and longevity. So, for scaling up the performances, MFCs can be constructed in different designs and configurations by selecting suitable material for anode and cathode (3). Three basic designs of MFC have been reported including single-chambered (SC), double-chambered (DC) and stacked (4). Among these designs DC- and SC-MFCs are generally used for wastewater management and electricity generation. Dual-chambered MFC comprises of two compartments: (i) an anaerobic anode, and (ii) an aerated cathode, which can be separated by either a proton exchange membrane or salt bridge (5). These membrane or salt bridges facilitate the flow of protons from anodic to cathode chamber (6). Proton exchange membrane produces more electricity as compared to a salt bridge which subsequently increases the cost of the instrument (7). In comparison to proton exchange membrane, salt bridge may be an alternative for the fabrication of simple and cost-effective MFC. Apart from design and fabrication, some other factors that affect the energy production and performance of MFC are electrolytes, microorganism, substrate, salts, pH and temperature (8,9).

Some bacteria have the ability to transfer the electrons extracellularly generated by the oxidation of organic compounds. Therefore, the electricity generated is directly related to the metabolic activity of the anodic bacteria (10). Several reports have authenticated the promising results for the use of prokaryotic microorganisms (11), while there are limited studies available on electrogenic capability of yeast. Yeast may be an ideal biocatalyst for MFC applications due to its nonpathogenic nature, ability to utilize a wide range of substrates, robustness, and easy handling (12). Only a few yeasts have been used in MFCs as biocatalyst, e.g., *Saccharomyces cerevisiae* (13), *Arxula adeninivorans* (14) and *Hansenula anomala* (11). Among various yeasts, *Pichia fermentans* is a nonpathogenic, safe and fast growing organism even under microaerophilic conditions, and widely used in beverage and food industries for flavor, aroma and fermentation process (15,16). Antagonistic properties of *P. fermentans* inhibit the growth of other fungi and bacteria, and increase the shelf life of beverage and food products (17). In context to the fuel cell, the antagonistic property of *P. fermentans* may help in preventing the growth of other contaminating microorganisms in the anodic chamber and hence may also produce better output voltage in contrast to other yeast cells.

Two major mechanisms for electron transport have been reported: (i) direct electron transfer and (ii) indirect electron transfer (18). Physical contact between the microbial cell and the anode is a major factor in direct electron transfer. In direct electron transfer, microorganisms contain membrane bound electron transport

* Corresponding author. Tel.: +91 141 3999100; fax: +91 141 3999102.
E-mail addresses: rakeshkumar.sharma@jaipur.manipal.edu, r.18sharma@gmail.com (R.K. Sharma).

1389-1723/$ – see front matter
https://doi.org/10.1016/j.jbiosc.2018.11.004

protein to transport the electrons from cytoplasm to its surrounding environment. These electrons are further received by anode. In contrast, indirect electron transfer is followed by many different mechanisms such as artificial redox mediators (exogenous) and primary and secondary metabolites. These mediators act as a vehicle for the transportation of electron to the anode (19,20). In MFC, microorganisms develop a biofilm on the anode surface by secreting extracellular polymeric substances (EPS). These EPS constituted of protein, polysaccharides, and extracellular DNA, which are involved in electron transfer (21). Thus, the study was designed to explore the exoelectrogenic properties of *P. fermentans* as a biocatalyst in fuel cell with and without exogenous mediator, methylene blue (MB), in a DC and SC membrane less bioreactors.

MATERIALS AND METHODS

Microorganism and inoculum preparation *P. fermentans* was procured from the Microbial Type Culture collection (MTCC 189) Chandigarh, India, and was cultured aerobically in yeast extract peptone dextrose (YEPD) agar. Actively growing culture (4–6 h) in YEPD broth at 28°C was used as an inoculum in the MFC.

Dual-chambered setup Dual-chambered MFC (Fig. 1A) was fabricated using glass flasks (working volume 150 mL) and operated in the presence (1.5 μM MB) or absence of mediator. Carbon fibers (100 cm length, 7 μm diameter) were used as anode and stainless steel wire (100 cm length, 0.05 mm diameter) as cathode. The electrodes were sterilized with 98% absolute ethanol, UV radiation and then rinsed by autoclaved distilled water, dried in aseptic conditions. YEPD broth medium was used as anolyte, while saline solution (0.01 % NaCl) was used as catholyte. Salt bridge (Tygon tubes inner diameter 3.2 mm containing 8 % NaCl and 3.5 % agar) was used to connect cathode and anode compartment for proton exchange. The salt bridge was sterilized with absolute alcohol, UV radiation and rinsed by autoclaved distilled water. Sterilized anode chamber was inoculated with 10 % (v/v) inoculum size and the MFCs were operated at room temperature (30 ± 2°C) for one month.

Single-chambered membrane less setup Single-chambered membrane less MFC (Fig. 1B) (working volume 100 mL YEPD broth) operated with mediator or without mediator. Carbon fibers anode and stainless steel wire cathode were placed vertically at a distance of 3 cm. The glass bottle was covered with rubber stopper. All other applicable parameters were same as DC setup. All experiments were performed in duplicates. Control experiment was done with both of the setups.

Electrochemical calculation Open circuit voltage (OCV) was recorded by a digital multimeter. The OCV and output voltage against external resistors ranging from 820 kΩ to 100 Ω for all the cells were recorded regularly. Polarization curves were obtained by changing the external resistance from 820 kΩ to 100 Ω at various time intervals.

Current I was calculated from Ohm's law $V = IR$, V as a cell voltage and R as the resistance. Similarly, power P is derived as the multiplication of V and I. Current and power densities (j and p, respectively) are calculated by the ratio of current and surface area of anode (carbon fibre) and power and surface area of anode, respectively. Internal resistance (R_{int}) is a major factor in the power density calculation which was calculated by $R_{int} = R\,(E/V-1)$ where R is external load, E is voltage of open circuit (voltage without any resistance) and output voltage with resistors (22). Cell potential (electromotive force, EMF) was recorded using Ag/AgCl reference electrode.

Cytotoxicity of MB To evaluate the toxicity level of MB against *P. fermentans* disc agar diffusion test was carried out. Sterile filter paper disks (5 mm) were soaked with variable concentrations, 1.5 μM, 3 μM or 6 μM of the MB. These discs were placed on yeast extract agar plates containing *P. fermentans* and incubated at 28°C for 48 h (23).

EPS production *P. fermentans* was grown in 100 mL sterilized YEPD broth and incubated for 12 days at 28°C. The aliquots were taken out at different time intervals (day 1, 2, 3, 9 and 12) to estimate EPS. Twenty milliliters of cell culture and a control was centrifuged simultaneously at 8000 rpm for 15 min. The supernatant was used for EPS estimation but in control experiment did not get any precipitation (EPS) to process further. Carbohydrate in EPS was estimated by phenol/sulfuric acid method (24). Glucose was used as a standard.

Fourier transform infrared spectroscopy Major functional groups of the EPS were detected by Fourier transform infrared (FTIR) spectroscopy. The sample was prepared by making a dry film on a glass slide using a drop of EPS solution.

RESULTS

Evaluation of MFC performance A gradual increase in the open cell voltage of all four types of reactors: (i) DC, (ii) DC with mediator (DCM), (iii) SC, and (iv) SC with mediator (SCM). OCV of the control setups were gradually decreased from 0.47 to 0.30 V within 2 days and further the value reduced to zero.

The absence of zones of inhibition around the samples suggested MB is non-toxic for cell, thus the presence of MB will not inhibit the yeast growth. The influence of MB on the *P. fermentans* cell performance was investigated in the form of current generation and power density.

Double-chambered MFC OCV is one of the important parameter to evaluate MFC performance. OCV response was recorded in both the reactors, DC and DCM was quite promising, which strengthen the exoelectrogenic potential of *P. fermentans* for various bioelectrochemical applications under microaerophilic conditions. MB positively influenced the cell performance by significantly enhancing the OCV and power density. EMF of the cell recorded against Ag/AgCl reference electrode was 0.902 V and 0.642 V for DCM and DC, respectively. Anode potential of DC setup was 0.343 V and 0.294 for mediatorless and mediated cell, respectively. Maximum OCV 0.60 V (day 15) and 0.488 V (day 24) was recorded for DCM and DC-MFC, respectively (Fig. 2). Day wise profiles of power density vs. current density were obtained by changing the external resistance (R) from 820 kΩ to 100 Ω. Maximum power density 1.23 μW cm^{-2} was recorded at 33 kΩ in DCM-MFC on day 17, which declined thereafter, whereas DC-MFC showed a maximum power density 0.407 μWcm^{-2} on day 25 (Fig. 3A, C). Output voltage of cell increased with different

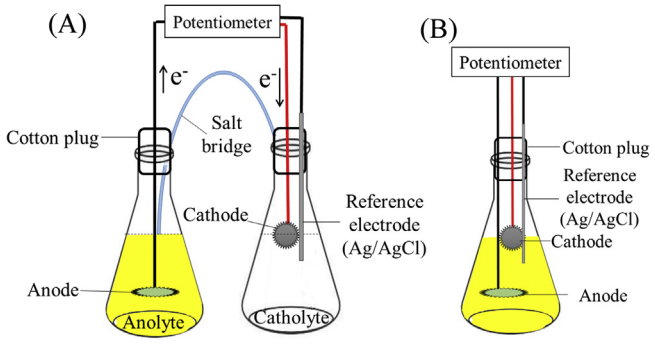

FIG. 1. Schematic representation of reactor design. (A) Double-chambered and (B) single-chambered.

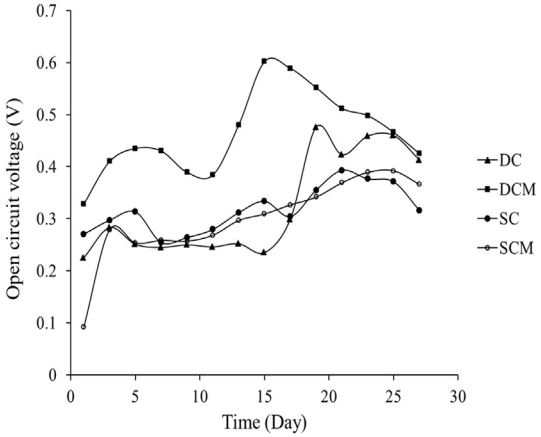

FIG. 2. Open circuit voltage during operation of fuel cell with *P. fermentans* as biocatalyst in single- and double-chambered: mediated and mediator less setups.

external resistance, current density decreased simultaneously. Maximum current density was recorded as 7.27 μAcm^{-2} and 18.18 μAcm^{-2} on day 25 and day 17 in DC and DCM setup, respectively (Fig. 3B, D).

Single-chambered setup Almost similar maximum OCVs of ~0.4 V (during 22–24 day) was recorded for both the cell setups (SCM and SC), while EMF of the cells (vs. Ag/AgCl reference electrode) was ~0.5 V. Anode potential of the mediated and mediatorless cell was 0.320 V and 0.206 V, respectively. As the OCV of both of the cells was very close but the power density and the current density of the reactors had significant difference. A maximum power density 1.64 μWcm^{-2} in SCM (day 25) and 0.643 μWcm^{-2} (day 21) in SC setup was observed across 10 kΩ (Fig. 4A, C). Current density 34.09 μA cm^{-2}and 40.90 μA cm^{-2} was achieved in SC and SCM, respectively (Fig. 4B, D). The lower OCV was compensated by large value of power density and current density. These values were dependent on the external resistance because output voltage increased with the increase in external load and current density decrease with the increase in output voltage. A gradual increase in external resistance also improved current generation. For current generation, external resistance acts as a limiting factor because all the other parameters have a slight influence. At the initial stage, there was no significant difference in power generation as sufficient electrons and protons were not generated till second day of experiment, while and after 2–3 days when a little up-shift of polarization curve was observed (Figs. 3A, C and 4A, C).

Internal resistance analysis The internal resistance (R_{int}) values for mediator containing reactors were almost similar up to 10 kΩ, which increased at higher external resistance. In SC, at the maximum resistance (180 kΩ), R_{int} gradually decreased from 314 kΩ to 57 kΩ from day 1 to day 25. In contrast, R_{int} of SCM increased from 50 kΩ to 72 kΩ at the maximum external resistance (180 kΩ) (Fig. 5A and B). In DC setup, internal resistance of DC decreased from 182 kΩ to 112 kΩ from day 1 to day 25. Lowest R_{int} value, 81 kΩ was recorded in DC on day 17. On the other hand, in DCM internal resistance increased from day 1 to day 25 from 115 kΩ to 175 kΩ at 180 kΩ external load, while the lowest impedence (52 kΩ) was recorded on day 21 (Fig. 5C and D).

Current discharge is basically a property of any battery through which represents the discharging rate of a cell. In this study, current discharge maximum observed in SCM which was 23 μA at 10 KΩ and lowest value of current discharge with time was 0.8 μA at 180 K in SC (Fig. 6). At 180 KΩ discharging was almost similar in all the setup.

EPS production Efficient EPS production was observed by *P. fermentans* along with its growth. However, a gradual decrease in EPS production after 9 days was recorded. The biofilm developed along with the surface of anode as well as at the top of medium. EPS production was well correlated with yeast growth. In the beginning, cells grow rapidly and biomass accumulation occurred, thus from day 1 to day 3 cell biomass, EPS and carbohydrate content in EPS was continuously increased (Fig. 7).

FTIR analysis of EPS Infrared (IR) spectrum of EPS confirms the presence of polysaccharide-protein matrix. During initial days, EPS production was minimum, which was also reflected in the IR spectrum as it did not show any significant peak for specific groups; however some emerging peaks at 1500 cm^{-1} and 3500–3700 cm^{-1} were noticed (Fig. 8). Two significant broad peaks ranged between 880 and 890 cm^{-1}and 744–748 cm^{-1} are assigned to C–H out-of-plane. During 3–6 days, functional groups representing primary amide (1691 cm^{-1}, 1644 cm^{-1}, C=O, –CONH$_2$) and secondary amide (1515 cm^{-1} was associated with ring vibration in the phenols of the tyrosine side-chains in and carbonyl stretch C = O of esters at 1741 cm^{-1} were observed (25). Beside this, it was also observed at 2360 cm^{-1} which corresponds to CO_2 (C=C=C, C=C=O, C≡C). Dong et al. (26) observed almost similar IR pattern in the

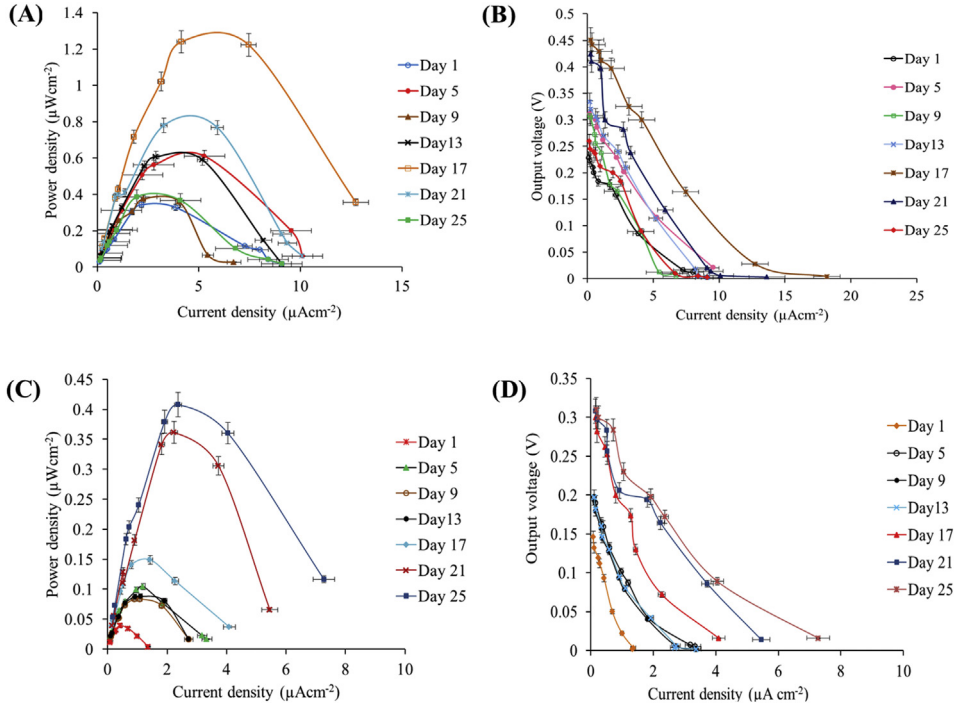

FIG. 3. Polarization curves of double-chambered setup; Current density vs power density (A) and current density vs output voltage (B) in mediator less setup, and current density vs power density (C) and current density vs output voltage (D) in mediated setup.

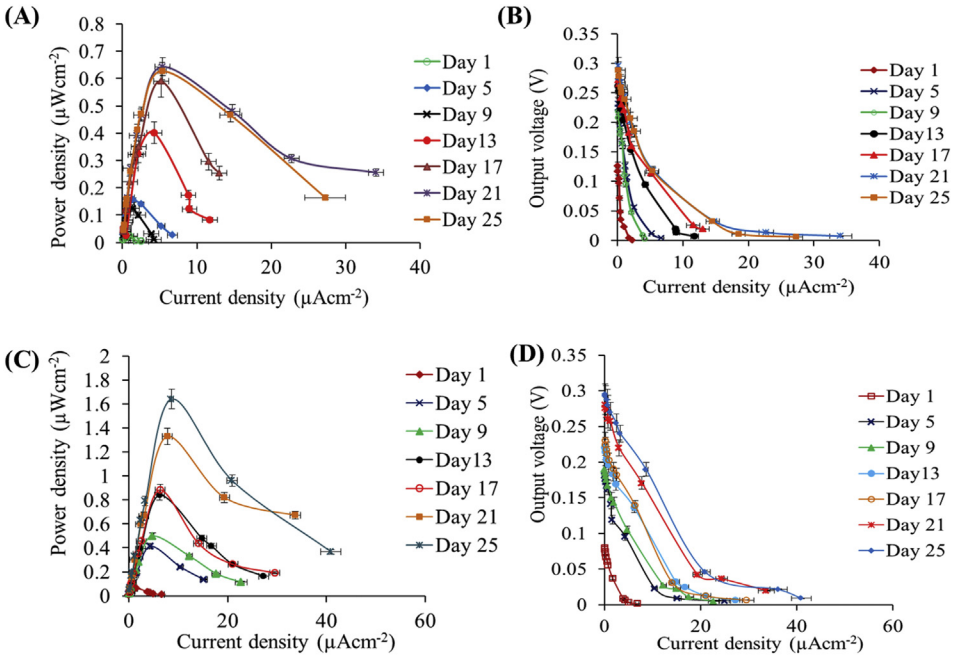

FIG. 4. Polarization curves of single-chambered setup; Current density vs. power density (A), current density vs output voltage (B) in mediator less setup and current density (C) and current density vs output voltage (D) in mediated setup.

EPS obtained from granulation of aerobic sludge. Li et al. (27) well reported the redox potential of bacterial EPS, which showed almost similar characteristic peaks regarding the presence of amide groups. Presence of tyrosine in EPS indicates its involvement in redox reactions (28).

A peak at 3618 cm^{-1} shows O—H hydroxyl groups in EPS. The region 3200—3000 cm^{-1} shows C—H stretch, whereas the bands in the region of 3000—2800 cm^{-1} indicates symmetric and anti-symmetric C—H stretching modes in the methyl (CH_3) and methylene (CH_2) functional groups. The region 1200—800 cm^{-1} is reported for polysaccharide; this region is dominated by ring vibrations overlapped with stretching vibrations of (C—OH) side groups and (C—O—C) glycosidic band vibration (29).

DISCUSSION

Reactor designs significantly influenced the performance of fuel cells. Maximum current density and power density were

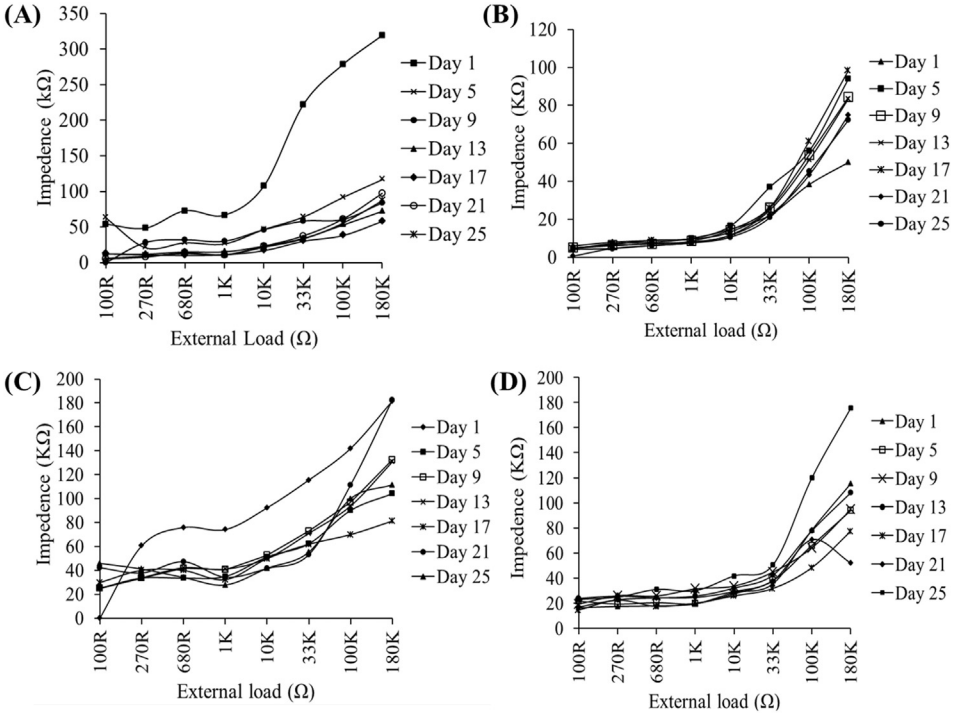

FIG. 5. Internal resistance of fuel cell at different external loads: SC (A), SCM (B), DC (C) and DCM (D).

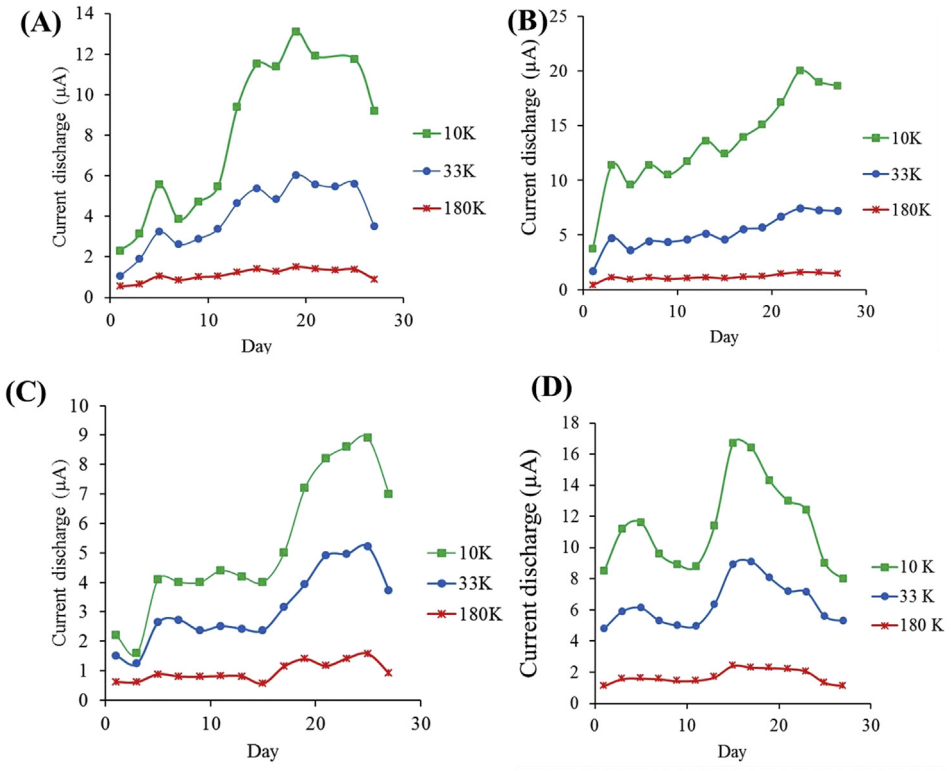

FIG. 6. Profile of Current discharge with time at different external resistance 10 KΩ, 33 KΩ and 180 KΩ in all four setup: SC (A), SCM (B), DC (C) and DCM (D).

statistically significantly higher ($P < 0.05$) in SC reactor designs. Earlier studies demonstrated that the endogenous mediator plays important role in the electron transfer from NADH and $FADH_2$ to the cellular membrane. These mediators diffuses in the thick cellular membrane and deliver these electrons to external electron acceptor such as oxygen (19). It was further reported that a maximum possible number of proton and electrons taken-up by endogenous mediators were 20 mol and 2 electrons for each NADH molecule. This completes the process of electron transfer in yeast cells attached to the anode surface by weak electrostatic interaction (30). This mechanism could be a reason of lower power and current density in DC and SC.

Addition of MB increased the cell performance, which revealed that MB acted as exogenous mediator for electron transport in these setups. The present observations are in consent with earlier studies that artificial mediators (MB, methyl orange, methyl red and neutral red) significantly promoted the electron generation thus improved the current generation by transferring the electron to anode surface (23,31). Christwardana et al. (30) reported that MB enters inside the cellular membrane and reduces to capture the 24 mol of electron and protons from glycolysis. These electrons are further delivered to the surface of anode whereas reduced MB converted into oxidized form.

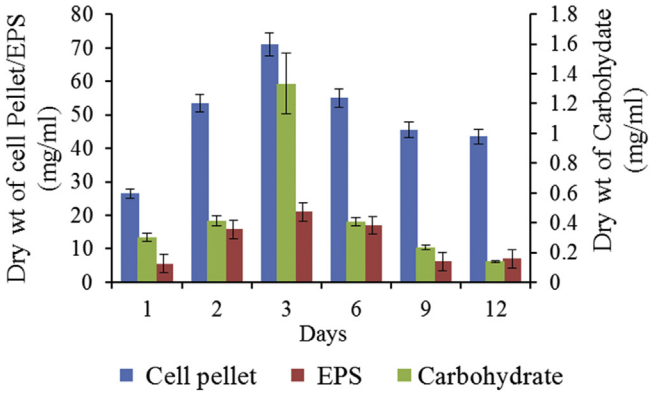

FIG. 7. Cell biomass and EPS content at different time interval.

Internal resistance negatively affects the current generation. R_{int} can be reduced by increasing the surface area of anode, cathode, proton exchange membrane, pH and ionic strength of electrolyte (32). In the case of SCM and DCM, internal resistance did not show significant difference up to 10 kΩ external load, while it increased at higher external load. At the lower external loads the R_{int} was significantly lower in the mediator containing reactors (R_{int} ranging from 10 to 30 Ω) as compared to mediator less reactors (R_{int} ranging from 10 to 70 Ω) during different days. This observation confirmed that mediators also play an important role in current generation and internal resistance. Earlier, similar observations were also reported with different exogenous mediators including MB and neutral red (33). *P. fermentans* produced EPS but did not form a dense biofilm on carbon fiber anode, which may limit direct electron transfer. However, its endogenous EPS and artificial mediator boosted the electron transfer via the indirect mechanism (19). Studies suggested that the combination of the two strategies, the attachment of yeast cells to the anode through amine or hydrogen bonds to improve the electron transfer directly and the use of a dissolved mediator to harvest electrons from floating cells, can be attempted to maximize a synergistic effect (34). This was facilitated by the surface modification of electrode with amine-based compounds and may induce physical entrapment, weak electrostatic interactions, and chemical bonding with yeast.

EPS comprises of polysaccharides, a variety of proteins, glycoproteins, glycolipids, and extracellular DNA. This EPS plays some important roles in microbial cell to cell communication, protection from external stress (such as toxic compounds, temperature) and extracellular electron transfer (35). Electron

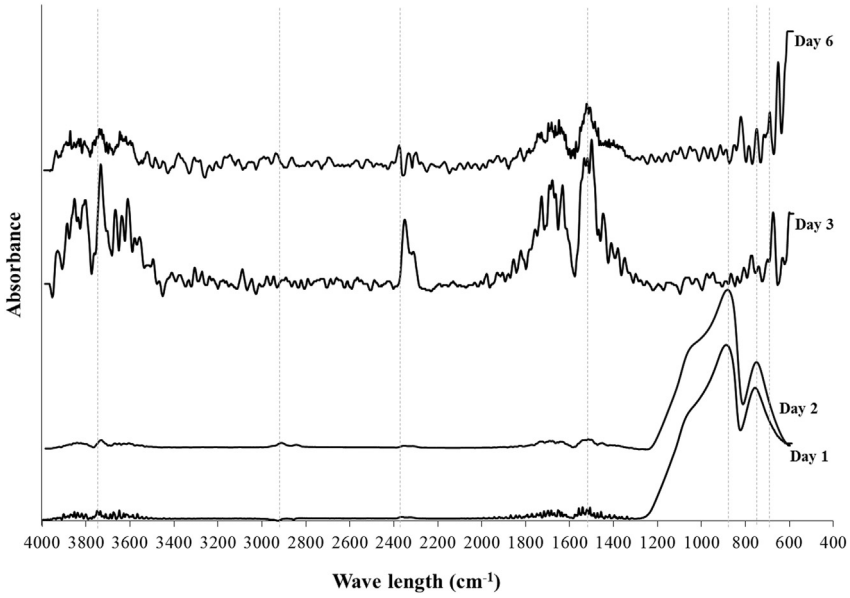

FIG. 8. FTIR spectra of EPS at different time interval.

hopping was proposed to be the most likely molecular mechanism for electrochemical electron transfer through EPS (36). Carbohydrate in EPS performs specific functions in microbial community and biofilm formation (37). Read and Costerton (38) reported that EPS production is an advantageous feature of microbes because it provides the strength of adhesive bond and also produce a protective glycocalyx. It also acts as mediator for transfer of electrons from yeast to anode as it might be involved in redox reactions (27), even when the cells are not actively producing the EPS. Once produced, it does not completely exert and may be involved in electron transfer.

Conclusion Power and current generation at moderate temperature under microaerophilic condition was well demonstrated by *P. fermentans* in different fuel cell setup. Endogenous EPS showed the presence of saccharides, protein having several functional groups like C—OH, COC, NH_2 and C=O, which strengthened the electron transfer property of *P. fermentans*. In DC design, the power density and current density were significantly higher in the presence of exogenous mediator (MB). This indicated towards the active role of MB to intensify the process. Overall, reactor designs also influenced power generation as the proposed SC membrane-less design showed better output as compared to the DC. This setup provides easy, economic and efficient design for various fuel cell applications. The results further point towards the potential of *P. fermentans* for its use in development of yeast based fuel cell.

ACKNOWLEDGMENT

Manipal University Jaipur is acknowledged for providing Enhanced Seed Grant (EF/2017-18/QE04-10) to Dr. R. K. Sharma and financial assistance to Ms. M. Pal for her research work.

References

1. **Kumar, R., Singh, L., Zularisam, A., and Hai, F. I.:** Microbial fuel cell is emerging as a versatile technology: a review on its possible applications, challenges and strategies to improve the performances, Int. J. Energy Res., **42**, 369—394 (2018).
2. **Rabaey, K. and Verstraete, W.:** Microbial fuel cells: novel biotechnology for energy generation, Trends Biotechnol., **23**, 291—298 (2005).
3. **Janicek, A., Fan, Y., and Liu, H.:** Design of microbial fuel cells for practical application: a review and analysis of scale-up studies, Biofuels, **5**, 79—92 (2014).
4. **Karmakar, S., Kundu, K., and Kundu, S.:** Design and development of microbial fuel cells, pp. 1029—1034, in: Méndez-Vilas, A. (Ed.), Current research, technology and education topics in applied microbiology and microbial biotechnology, vol. 1. Formatex Research Center, Badajoz (2010).
5. **Khan, M. R., Bhattacharjee, R., and Amin, M. S. A.:** Performance of the salt bridge based microbial fuel cell, Int. J. Eng. Technol., **1**, 78 (2012).
6. **Min, B., Cheng, S., and Logan, B. E.:** Electricity generation using membrane and salt bridge microbial fuel cells, Water Res., **39**, 1675—1686 (2005).
7. **Asensio, Y., Fernandez-Marchante, C. M., Lobato, J., Cañizares, P., and Rodrigo, M. A.:** Influence of the ion-exchange membrane on the performance of double-compartment microbial fuel cells, J. Electroanal. Chem., **808**, 427—432 (2018).
8. **Kuppam, C., Kadier, A., Kumar, G., Nastro, R., and Jeevitha, V.:** Challenges in microbial fuel cell and future scope, pp. 483—499, in: Das, D. (Ed.), Microbial fuel cell. Springer, Cham (2018).
9. **Aghababaie, M., Farhadian, M., Jeihanipour, A., and Biria, D.:** Effective factors on the performance of microbial fuel cells in wastewater treatment — a review, Environ. Technol. Rev., **4**, 71—89 (2015).
10. **Choi, S.:** Microscale microbial fuel cells: advances and challenges, Biosens. Bioelectron., **69**, 8—25 (2015).
11. **Logan, B. E.:** Exoelectrogenic bacteria that power microbial fuel cells, Nat. Rev. Microbiol., **7**, 375—381 (2009).
12. **Walker, A. L. and Walker, C. W., Jr.:** Biological fuel cell and an application as a reserve power source, J. Power Sources, **160**, 123—129 (2006).
13. **Sayed, E. T. and Nakagawa, N.:** Critical issues in the performance of yeast based microbial fuel cell, J. Chem. Technol. Biotechnol., **93**, 1588—1594 (2018).
14. **Haslett, N. D., Rawson, F. J., Barrière, F., Kunze, G., Pasco, N., Gooneratne, R., and Baronian, K. H.:** Characterisation of yeast microbial fuel cell with the yeast *Arxula adeninivorans* as the biocatalyst, Biosens. Bioelectron., **26**, 3742—3747 (2011).
15. **Mingorance-Cazorla, L., Clemente-Jiménez, J. M., Martínez-Rodríguez, S., Las Heras-Vázquez, F. J., and Rodríguez-Vico, F.:** Contribution of different natural yeasts to the aroma of two alcoholic beverages, World J. Microbiol. Biotechnol., **19**, 297—304 (2003).
16. **Ravasio, D., Carlin, S., Boekhout, T., Groenewald, M., Vrhovsek, U., Walther, A., and Wendland, J.:** Adding flavor to beverages with non-conventional yeasts, Fermentation, **4**, 15 (2018).
17. **Aladdin, A., Dib, J. R., Malek, R. A., and El Enshasy, H. A.:** Killer yeast, a novel biological control of soilborne diseases for good agriculture practice, pp. 71—86, in: Zakaria, Z. (Ed.), Sustainable technologies for the management of agricultural wastes. Springer, Singapore (2018).
18. **Schroder, U.:** Anodic electron transfer mechanisms in microbial fuel cells and their energy efficiency, Phys. Chem. Chem. Phys., **9**, 2619—2629 (2007).
19. **Hubenova, Y. and Mitov, M.:** Extracellular electron transfer in yeast-based biofuel cells: a review, Bioelectrochemistry, **106**, 177—185 (2015).
20. **Hubenova, Y., Hubenova, E., Slavcheva, E., and Mitov, M.:** The glyoxylate pathway contributes to enhanced extracellular electron transfer in yeast-based biofuel cell, Bioelectrochemistry, **116**, 10—16 (2017).

21. **Donlan, R. M.:** Biofilms: microbial life on surfaces, Emerg. Infect. Dis., **8**, 881–890 (2002).
22. **Logan, B. E., Hamelers, B., Rozendal, R., Schröder, U., Keller, J., Freguia, S., Aelterman, P., Verstraete, W., and Rabaey, K.:** Microbial fuel cells: methodology and technology, Environ. Sci. Technol., **40**, 5181–5192 (2006).
23. **Babanova, S., Hubenova, Y., and Mitov, M.:** Influence of artificial mediators on yeast-based fuel cell performance, J. Biosci. Bioeng., **112**, 379–387 (2011).
24. **Dubois, M., Gilles, K. A., Hamilton, J. K., Rebers, P. T., and Smith, F.:** Colorimetric method for determination of sugars and related substances, Anal. Chem., **28**, 350–356 (1956).
25. **Barth, A.:** The infrared absorption of amino acid side chains, Prog. Biophys. Mol. Biol., **74**, 141–173 (2000).
26. **Dong, J., Zhang, Z., Yu, Z., Dai, X., Xu, X., Alvarez, P. J. J., and Zhu, L.:** Evolution and functional analysis of extracellular polymeric substances during the granulation of aerobic sludge used to treat p-chloroaniline wastewater, Chem. Eng. J., **330**, 596–604 (2017).
27. **Li, S.-W., Sheng, G.-P., Cheng, Y.-Y., and Yu, H.-Q.:** Redox properties of extracellular polymeric substances (EPS) from electroactive bacteria, Sci. Rep., **6**, 39098 (2016).
28. **Warren, J. J., Winkler, J. R., and Gray, H. B.:** Redox properties of tyrosine and related molecules, FEBS Lett., **586**, 596–602 (2012).
29. **Wiercigroch, E., Szafraniec, E., Czamara, K., Pacia, M. Z., Majzner, K., Kochan, K., Kaczor, A., Baranska, M., and Malek, K.:** Raman and infrared spectroscopy of carbohydrates: a review, Spectrochim. Acta A Mol. Biomol. Spectrosc., **185**, 317–335 (2017).
30. **Christwardana, M., Frattini, D., Accardo, G., Yoon, S. P., and Kwon, Y.:** Effects of methylene blue and methyl red mediators on performance of yeast based microbial fuel cells adopting polyethylenimine coated carbon felt as anode, J. Power Sources, **396**, 1–11 (2018).
31. **Rahimnejad, M., Najafpour, G. D., Ghoreyshi, A. A., Shakeri, M., and Zare, H.:** Methylene blue as electron promoters in microbial fuel cell, Int. J. Hydrogen Energy, **36**, 13335–13341 (2011).
32. **Fan, Y., Sharbrough, E., and Liu, H.:** Quantification of the internal resistance distribution of microbial fuel cells, Environ. Sci. Technol., **42**, 8101–8107 (2008).
33. **Taskan, E., Özkaya, B., and Hasar, H.:** Effect of different mediator concentrations on power generation in MFC using Ti-TiO_2 electrode, Int. J. Energy Sci., **4**, 9–11 (2014).
34. **Chung, Y., Ahn, Y., Christwardana, M., Kim, H., and Kwon, Y.:** Development of a glucose oxidase-based biocatalyst adopting both physical entrapment and crosslinking, and its use in biofuel cells, Nanoscale, **8**, 9201–9210 (2016).
35. **Flemming, H.-C., Neu, T. R., and Wozniak, D. J.:** The EPS matrix: the "house of biofilm cells", J. Bacteriol., **189**, 7945–7947 (2007).
36. **Xiao, Y., Zhang, E., Zhang, J., Dai, Y., Yang, Z., Christensen, H. E., Ulstrup, J., and Zhao, F.:** Extracellular polymeric substances are transient media for microbial extracellular electron transfer, Sci. Adv., **3**, e1700623 (2017).
37. **Davey, M. E. and O'toole, G. A.:** Microbial biofilms: from ecology to molecular genetics, Microbiol. Mol. Biol. Rev., **64**, 847–867 (2000).
38. **Read, R. and Costerton, J.:** Purification and characterization of adhesive exopolysaccharides from *Pseudomonas putida* and *Pseudomonas fluorescens*, Can. J. Microbiol., **33**, 1080–1090 (1987).